Combustion of Methane over Palladium-Based Catalysts: Catalytic Deactivation and Role of the Support

ARTICLE *in* THE JOURNAL OF PHYSICAL CHEMISTRY C · APRIL 2012

Impact Factor: 4.77 · DOI: 10.1021/jp212236e

3 AUTHORS, INCLUDING:

William R. Schwartz
Yale University
9 PUBLICATIONS **162** CITATIONS
SEE PROFILE

Dragos Ciuparu
Petroleum - Gas University of Ploiesti
69 PUBLICATIONS **2,055** CITATIONS
SEE PROFILE

THE JOURNAL OF PHYSICAL CHEMISTRY C

Article

pubs.acs.org/JPCC

Combustion of Methane over Palladium-Based Catalysts: Catalytic Deactivation and Role of the Support

William R. Schwartz,*[,†] Dragos Ciuparu,[‡] and Lisa D. Pfefferle[†]

[†]Department of Chemical Engineering, Yale University, New Haven, Connecticut 06520, United States

[‡]Universitatea Petrol-Gaze Ploiesti, Ploiesti, Romania

Supporting Information

ABSTRACT: Palladium-based catalysts supported on metal oxides are attractive for methane combustion at low temperature. However, at temperatures below 450 °C, their tendency to deactivate hinders their usefulness. Catalytic deactivation in this temperature regime has been attributed to a water/hydroxyl inhibition effect. We investigated this effect to better understand the mechanism for catalytic deactivation. Comparative in situ FTIR transmission spectroscopy experiments at 325 °C revealed that hydroxyl accumulation occurs on the oxide supports during catalytic methane combustion and deactivation. The water/hydroxyl accumulation on the support is slow to desorb at this temperature. In light of our recent finding that oxygen from the support is utilized in the methane combustion process, we propose that hydroxyl/water accumulation on the support impedes the catalytic combustion reaction by hindering oxygen mobility on the support. We support this hypothesis by demonstrating that the presence of water on the catalyst inhibits oxygen exchange with the oxide support.

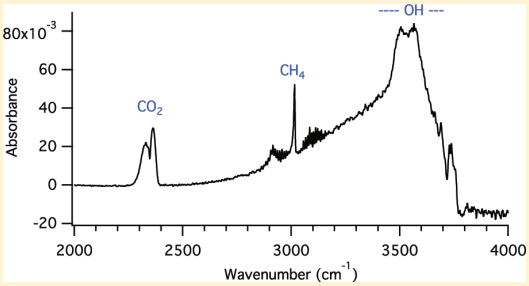

INTRODUCTION

Catalytic deactivation of the methane oxidation reaction over palladium-based catalysts is of interest and has been extensively studied, due to the otherwise attractive potential for catalytic combustion. In the low temperature regime below 450 °C, a leading hypothesis for catalytic deactivation is water poisoning of the catalyst surface by the formation of $Pd(OH)_2$.[1−5] Though it has been generally accepted that water poisoning of the catalyst surface plays a role in catalytic deactivation, no agreement on the mechanism for catalytic deactivation has been attained.

The influence of water on the rate of reaction for methane oxidation over supported Pd catalysts has been shown to be generally around negative first order in the low temperature regime.[3,6] Each of these experimenters used an external source of water in the feed to determine the kinetic impact of water on the catalytic methane combustion reaction. A subsequent study by Ciuparu et al.[7] suggested that hydroxyl groups resulting from methane dissociation are likely to be more strongly bound to the catalyst surface relative to adsorbed hydroxyls from an external water source. Therefore, measurements of water adsorption/desorption kinetics based on an external water source may be misleading.

The inhibition effect due to water is known to be temperature dependent. Ciuparu et al.[8] showed that the reaction order with respect to water concentration varied from −1 at 300 °C to 0 at 500 °C. Likewise, Burch et al.[9] demonstrated in their study that water inhibition was significant up to about 450 °C. This is the temperature at which the desorption time gap between the CO_2 and water has been shown to disappear.[7] The desorption time gap refers to the delay between CO_2 and water production on the Pd catalyst surface, and their subsequent detection by gas phase mass spectrometry. Ciuparu et al.[7] found that, at temperatures below 450 °C, CO_2 product from catalytic methane combustion was detected more quickly than water, suggesting that water was accumulating on the catalyst surface. At 450 °C and higher temperatures, water was detected as quickly as CO_2, indicating that water accumulation on the catalyst surface was no longer occurring.

The water inhibition effect is also dependent on the type of support. Oxygen mobility on the support has been found to potentially influence catalytic reaction inhibition by water. In a study of PdO/Al_2O_3, PdO/ZrO_2, and $PdO/Ce_{.1}Zr_{.9}O_2$, Ciuparu et al.[10] found that the greater the support's oxygen surface mobility (Al_2O_3 < ZrO_2 < $Ce_{.1}Zr_{.9}O_2$), the greater the resistance to water inhibition of the catalytic reaction.

Since the formation and accumulation of $Pd(OH)_2$ is a leading theory for catalytic deactivation, we looked extensively for definitive evidence of Pd−OH bonding on a variety of PdO-based catalysts during methane combustion. Our recent study of the catalytic combustion reaction mechanism[11] suggests that an alternative cause for catalytic deactivation is hydroxyl/water accumulation on the oxide support, which blocks oxygen

Received: December 19, 2011
Revised: March 15, 2012

   dx.doi.org/10.1021/jp212236e | J. Phys. Chem. C XXXX, XXX, XXX−XXX

surface migration from the support to active catalytic sites. Therefore, in this study, we looked for a correlation between hydroxyl/water accumulation on the support and oxygen surface mobility, as measured by the rate of oxygen exchange between the gas phase and the support.

EXPERIMENTAL SECTION

Catalysts used in this investigation were 3 wt % PdO/Al_2O_3, 3 wt % PdO/MgO, 3 wt % PdO/TiO_2, and 3 wt % PdO/MCM-41. Each catalyst was prepared by incipient wetness impregnation with a $Pd(NO_3)_2{\cdot}2H_2O$ precursor. Palladium nitrate dihydrate was dissolved in aqueous HNO_3 (pH 1.3) and then impregnated onto the metal oxide supports. The materials were dried overnight at room temperature and were subsequently calcined in air for four hours. The PdO/MCM-41 sample was calcined at 550 °C, and other samples were each calcined at 450 °C.

Catalyst Characterization. The oxide supports were characterized by N_2 physisorption, and the PdO catalysts were characterized by temperature programmed reduction (TPR), transmission electron microscopy (TEM), and X-ray diffraction (XRD).

Temperature programmed reduction was performed with a gas chromatograph (GC) using a thermal conductivity detector to monitor H_2 consumption. The carrier gas was 5% H_2 in Ar. Palladium oxide on three of the four supports reduced in H_2 near room temperature. Consequently, the sample cell was cooled with liquid N_2 boil-off gas prior to starting TPR.

Description of Experiments. To test for hydroxyl accumulation on PdO and on the supports during catalytic deactivation, we utilized in situ transmission FTIR spectroscopy at 325 °C. This temperature was sufficiently high to observe CH_4 conversion to CO_2 and H_2O, yet low enough to also observe catalytic deactivation associated with water accumulation.[8,9]

To distinguish activity on the PdO surface from activity on the support, we tested the PdO catalyst loaded on four unique metal oxide supports: Al_2O_3, MgO, TiO_2, and MCM-41. Since PdO is the only common material among the tested catalysts, a common hydroxyl vibrational peak among the supported catalysts would provide evidence of Pd−OH bond formation, provided that each of these unique supports have unique hydroxyl vibrational frequencies. The absence of a common hydroxyl peak would suggest either that there is no significant accumulation of Pd−OH bonds during methane combustion and catalytic deactivation or that the ratio of PdO to the support is so small that hydroxyl accumulation on PdO is not distinguishable from hydroxyls on the support, due to interference from broad OH peaks on the support.

FTIR time series transmission experiments were performed with a Nicolet Nexus 870 using an MCT/A detector with a resolution of 4 cm^{-1}, 32 scans per data set, aperture setting of 100, and mirror velocity of 2 cm/sec. Pellets of the catalyst were placed in a reactor cell with CaF_2 windows at each end to allow the IR beam to pass through the enclosed catalyst pellet.

Two mixture gas cylinders provided the reactants to the catalyst. One cylinder was composed of 4% O_2 in He, while the other cylinder contained a mixture of 1% CH_4 plus 4% O_2 in He.

The PdO-based catalysts were all pretreated by flowing the O_2/He mixture through the reactor cell at 35 mL/min, while it was heated to 450 at 5 °C/min and held at that temperature for 2 h. This allowed water, CO_2, and other impurities to desorb from the catalyst surface. The reactor cell was then cooled to the desired reaction temperature.

To minimize atmospheric water vapor and CO_2 from interfering with experimental tests, the FTIR apparatus was connected to a high pressure liquid N_2 tank from which N_2 boil-off continuously flowed inside the FTIR apparatus at 10 standard cubic feet per hour (SCFH).

The in situ FTIR time series spectroscopy experiments were conducted over a 40 min period. During the first 20 min, the 1% CH_4/4% O_2/95% He mixture flowing at 5 mL/min was added to the existing 4% O_2 in He gas flow. This resulted in a total gas flow of 40 mL/min, with an equivalence ratio of 0.1 ($\text{fuel-to-oxygen}_{\text{actual}}/\text{fuel-to-oxygen}_{\text{stoichiometric}}$). During the next 20 min period, the reactant mixture was switched off, while the 4% O_2 in He mixture continued to flow at 35 mL/min. By obtaining time series spectra both during and postreaction, we were able to monitor CH_4 conversion plus the rates of hydroxyl, CO_2, and CH_4 accumulation and subsequent desorption.

As an additional test to determine if Pd−OH bonds accumulate during catalytic methane combustion and deactivation, we used isotopic oxygen to distinguish hydroxyl accumulation on Pd from hydroxyl accumulation on the support. We used in situ FTIR spectroscopy at 250 °C with CH_4 + $^{16}O_2$ flowing over $Pd^{18}O/Al_2{}^{16}O_3$, and $Pd^{16}O/Al_2{}^{16}O_x{}^{18}O_{(3-x)}$ to analyze hydroxyl IR vibrational peak shifts associated with the presence of ^{18}O on the catalyst material. We also used in situ FTIR spectroscopy with CH_4 + $^{16}O_2$ flowing over $Pd^{16}O$/MCM-41 and $Pd^{18}O$/MCM-41 at 325 °C to similarly determine if a hydroxyl IR vibrational peak shift could be observed and attributed to $Pd(OH)_2$ under our experimental conditions. For each of these catalysts, the presence of ^{18}O in hydroxyl groups on the catalyst surface causes a vibrational downward energy shift compared to hydroxyls containing ^{16}O. Isotopic oxygen is calculated to cause a vibrational energy shift of about 12 cm^{-1} in the absence of other influencing factors. Hydrogen bonding hydroxyls to the catalyst surface will reduce the magnitude of the vibrational energy shift. We tested for the magnitude of expected vibrational shifts caused by the presence of isotopic oxygen under our experimental conditions, finding a vibrational shift of around 7 cm^{-1} when CH_4 plus $^{18}O_2$ flowed over $Pd^{18}O/Al_2{}^{16}O_x{}^{18}O_{(3-x)}$. This data is presented in the Supporting Information. If $Pd(OH)_2$ was accumulating during methane combustion and catalytic deactivation, we would expect to see a similar downward vibrational shift on our $Pd^{18}O$-based catalysts.

$Pd^{18}O/Al_2{}^{16}O_3$ and $Pd^{18}O$/MCM-41 were prepared by reducing the PdO to Pd metal in fresh $Pd^{16}O/Al_2{}^{16}O_3$ and $Pd^{16}O$/MCM-41, and then reoxidizing the metal with $^{18}O_2$. To reduce PdO and not Al_2O_3 and MCM-41, 5% H_2 in He flowed over the catalysts at 300 °C for one hour. Ultra high purity He subsequently flowed for one hour to remove excess H_2 from the reactor and to desorb water formed during the reduction process. The Pd metal on Pd/Al_2O_3 was then reoxidized at 300 °C with 4% $^{18}O_2$ in He purchased from Isotec Corporation that was certified as 99% pure. We previously observed that oxygen exchange with PdO/Al_2O_3 does not become significant until about 380 °C.[11] Oxygen exchange on the catalysts was conducted at only 300 °C in order to prevent oxygen exchange with the support.

The $Pd^{16}O/Al_2{}^{16}O_x{}^{18}O_{(3-x)}$ catalyst was prepared by first heating $Pd^{16}O/Al_2{}^{16}O_3$ to 550 °C and flowing 4% $^{18}O_2$ in He for 2 h. The temperature of 550 °C is a high enough

dx.doi.org/10.1021/jp212236e | J. Phys. Chem. C XXXX, XXX, XXX−XXX

temperature to partially exchange oxygen on both $Pd^{16}O$ and the $Al_2{}^{16}O_3$ support with gas phase $^{18}O_2$, producing $Pd^{18}O_x{}^{16}O_{(1-x)}/Al_2{}^{16}O_x{}^{18}O_{(3-x)}$.[11,18] The reactor temperature was then reduced to 275 °C. $^{18}O_2$ gas flow was stopped, while pure He continued to flow. After $^{18}O_2$ gas was purged from the reactor, 5% H_2 in He as added to the existing He flow for about 20 min, causing $Pd^{18}O_x{}^{16}O_{(1-x)}/Al_2{}^{16}O_x{}^{18}O_{(3-x)}$ to reduce Pd metal/$Al_2{}^{16}O_x{}^{18}O_{(3-x)}$. The Pd metal was then reoxidized with 4% $^{16}O_2$ in He, resulting in $Pd^{16}O/Al_2{}^{16}O_x{}^{18}O_{(3-x)}$. In our related study,[11] we tested for the possibility of oxygen scrambling between Pd and the support during our synthesis process. Temperature programmed oxidation with $^{18}O_2$ over $Pd/Al_2{}^{16}O_3$ revealed that there is no significant oxygen scrambling between Pd−O and the support oxide under our synthesis conditions.[11]

Prior to reaction, the isotopically labeled alumina-based catalysts were heat treated at 275 °C in UHP He for one hour, flowing at 35 mL/min. This low temperature heat treatment was used to prevent oxygen scrambling between PdO and the alumina support. The reactor temperature was then lowered to 250 °C, and the reaction was started by adding 5 mL/min mixture flow of 1% CH_4 and 4% $^{16}O_2$ in He to an existing 35 mL/min flow of UHP He.

For the MCM-41-based catalyst, we determined that oxygen exchange with Pd/MCM-41 becomes significant around 480 °C. This relatively high temperature at which oxygen exchange becomes significant is due to the low oxygen mobility associated with SiO_2. Consequently, we were able to heat treat this catalyst at higher temperature in comparison to the alumina based catalysts. $Pd^{18}O$/MCM-41 was heat treated at 430 °C for 1 h prior to reaction. The temperature was then lowered to 325 °C, where the methane combustion reaction was initiated with the same gas flows that were present during methane combustion over the alumina-based catalysts.

To better identify small vibrational shifts on these catalysts, we increased the FTIR resolution from 4 cm^{-1} to 2 cm^{-1} and decreased the aperture setting from 100 to 69. To compensate for increased noise in the FTIR spectra on the isotopically labeled samples, the number of scans per data set was increased from 32 to 128. Mirror velocity was unchanged at 2 cm/sec.

In our final set of experiments, we tested for a correlation between water poisoning of the catalyst support and the amount of oxygen exchange between the support and gas phase O_2. Catalysts for these experimental trials were $Pd^{18}O/Al_2{}^{16}O_3$ and $Pd^{18}O/Mg^{16}O$. A mixture of 4% $^{18}O_2$ in He flowing at 5 mL/min plus UHP He flowing at 35 mL/min flowed into a Pyrex tubular reactor containing the catalyst sample. The gas mixture flow continued from the reactor to a residual gas analyzer (RGA) mass spectrometer, and oxygen exchange with the support was measured by the appearance of $^{18}O^{16}O$.

The catalysts were heated to 400 °C, which is sufficiently high to observe isotopic oxygen exchange with the supports in the absence of methane reaction, yet within the temperature regime where catalytic deactivation occurs during methane combustion. It should be noted[11] that oxygen exchange with the support occurs at a lower temperature during the methane or hydrogen oxidation reaction. During the oxygen exchange reaction, about 3 μL of water were injected into the gas flow upstream from the reactor. Its subsequent impact on $^{18}O^{16}O$ production, which reflects oxygen surface mobility, was monitored by the RGA mass spectrometer.

RESULTS AND DISCUSSION

Catalyst Characterization. Catalyst characterization results, including comparative TEM particle size and distributions, XRD particle size estimates, TPR profiles, and physisorption data on the oxide supports are summarized in Table 1. The appropriate parameter from TEM particle size measurements for comparison with XRD crystallite particle size calculations is the volume weighed average diameter, d_v, where $d_v = \sum n_i d_i^4 / \sum n_i d_i^3$.[12] The XRD particle size was estimated from the Scherrer equation.[13] The PdO particle diameter estimates from TEM and XRD are consistent on each of the supports, with the exception of 3 wt % PdO/MCM-41, where XRD crystallite particle diameter is calculated to be around 5 nm; smaller than the diameter estimated from TEM. The difference may due to agglomerated particles measured on TEM images.

Table 1. Catalyst Characterization Data: Summary of Physisorption, TPR, XRD, and TEM Analysis

procedure	3 wt % PdO/Al_2O_3	3 wt % PdO/MgO	3 wt % PdO/TiO_2	3 wt % PdO/MCM-41
TEM average PdO particle diameter	11 ± 5 nm	12 ± 4 nm	11 ± 3 nm	9 ± 2 nm
TEM volume weighted average PdO particle diameter $d_v = \sum n_i d_i^4 / \sum n_i d_i^3$	17 ± 5 nm	15 ± 4 nm	14 ± 3 nm	11 ± 2 nm
XRD average PdO particle diameter	12 nm	13 nm	12 nm	6 nm
N_2 physisorption BET surface area of support	480 m^2/g	813 m^2/g	122 m^2/g	1,113 m^2/g
N_2 physisorption BJH pore volume of support	1.3 cc/g	0.82 cc/g	0.46 cc/g	1.4 cc/g
TPR: temperature at which peak reduction occurs	24 °C	66 °C	48 °C	40 °C

Catalyst Behavior during Methane Combustion and Deactivation. Figure 1 shows typical FTIR spectra for the four PdO-based catalysts with different oxide supports, illustrating that hydroxyl coverage is dependent on the support. Each of the spectra in Figure 1 was obtained during a methane combustion reaction at 325 °C, and each spectrum was taken at the same time frame, about 20 min into the methane combustion reaction. Methane conversion levels for three of the catalysts samples were similar: about 13% for PdO/MgO, 16% for PdO/TiO_2, and 21% for PdO/Al_2O_3. Methane conversion was lower, at about 4% over the PdO/MCM-41 catalyst. The lower conversion rate may be due to relatively smaller PdO crystallite size on the MCM-41 support (Table 1). In a study of the effect of Pd crystallite size on catalytic activity, Muller et al.[14] observed that, at reaction temperatures between 327 and 377 °C, smaller crystallite PdO particles are associated with lower catalytic activity. This was attributed to smaller PdO crystallite particles having greater contact with the support, which in turn limited PdO reducibility by methane. An additional cause for the lower catalytic activity on the 3 wt % PdO/MCM-41 catalyst is a higher concentration of hydroxyls on the MCM-41 catalyst after calcination, compared to the hydroxyl concentration on the other metal oxide supports after calcination. This is due to the higher energy required to desorb water from MCM-41 compared to the other metal oxide supports.

dx.doi.org/10.1021/jp212236e | J. Phys. Chem. C XXXX, XXX, XXX−XXX

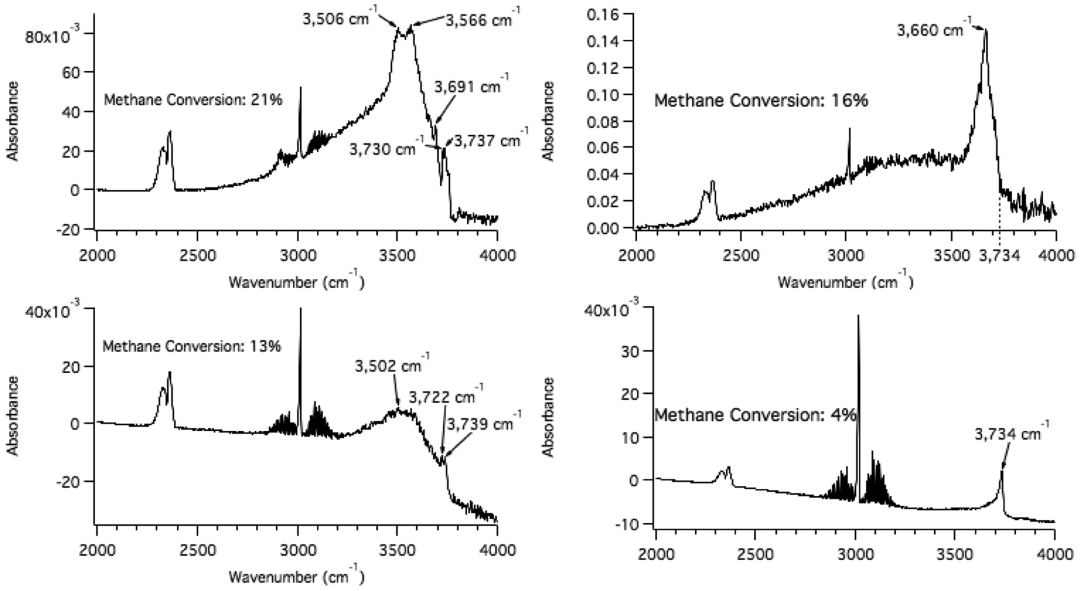

Figure 1. FTIR transmission spectra with 4 cm^{-1} resolution during methane combustion at 325 °C over the catalysts: 3 wt % PdO/Al_2O_3 (top left), 3 wt % PdO/TiO_2 (top right), 3 wt % PdO/MgO (bottom left), and 3 wt % PdO/MCM-41 (bottom right).

The double peak between 2280−2390 cm^{-1} represents CO_2. The middle peak centered at 3016 cm^{-1} represents CH_4. The hydroxyl region in the FTIR spectra extends from around 3200−3800 cm^{-1}. This typical broad range corresponds to weakly H-bonded surface hydroxyls bonded to the support.[19] The 3 wt % PdO/MCM-41 peak in the hydroxyl area is less broad, due in part to the lower conversion compared to conversion on the other catalysts, and shows only a single distinguishable peak at 3734 cm^{-1}, where the MCM-41 silanol peak exists at 325 °C.

In the hydroxyl region shown in Figure 1, there is no distinguishable common peak among all the catalysts, though there is signal at 3734 cm^{-1} for all samples. The large contribution of OH bonding on the supports covers the regions of Pd−OH bonding reported by other investigators.[5] Consequently, we show no definitive supporting evidence for $Pd(OH)_2$ formation. However, the small common IR signal around 3734 cm^{-1} may represent Pd−OH masked by nearby hydroxyl peaks on each of the supports.

Gao et al.[5] also used FTIR spectroscopy to find hydroxyl peaks on Pd/Al_2O_3. These authors found six hydroxyl peaks, attributing three of them, 3770, 3723, and 3680 cm^{-1}, to OH species on Al_2O_3, based on prior studies.[10,15,16] The remaining three low intensity peaks in their study, at 3556, 3697, and 3733 cm^{-1} were attributed to hydroxyl species on PdO.

It is possible that the peaks at 3556 and 3697 cm^{-1} identified and attributed to hydroxyls on PdO by Gao et al. represent hydroxyls that are bridged between Pd and their Al_2O_3 support, and that the higher energy peak at 3733 cm^{-1} represents a singular Pd−OH bond. To substantiate this, we performed FTIR spectroscopy during CH_4 + $^{16}O_2$ combustion over $Pd^{18}O/Al_2{}^{16}O_3$ and $Pd^{16}O/Al_2{}^{16}O_x{}^{18}O_{(3-x)}$. A downward IR vibrational energy shift would be expected for peaks associated with the accumulation of hydroxyls on Pd using the $Pd^{18}O/Al_2{}^{16}O_3$ catalyst in comparison with the $Pd^{16}O/Al_2{}^{16}O_x{}^{18}O_{(3-x)}$ catalyst. Likewise, a downward IR vibrational energy shift would be expected for peaks associated with the accumulation of hydroxyls on alumina using the $Pd^{16}O/Al_2{}^{16}O_x{}^{18}O_{(3-x)}$ catalyst in comparison to the $Pd^{18}O/Al_2{}^{16}O_3$ catalyst. The results of these in situ spectrometry trials are shown in Figure 2.

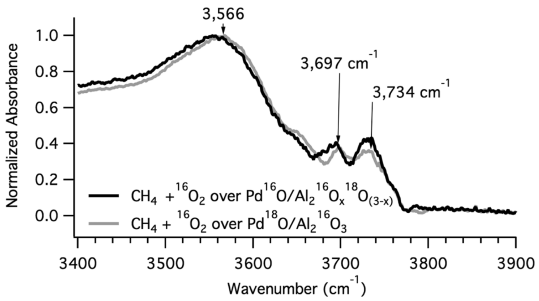

Figure 2. FTIR transmission spectra with 2 cm^{-1} resolution in the hydroxyl region during methane combustion over isotopic oxygen labeled 3 wt % PdO/Al_2O_3 at 250 °C.

The broad peak at 3566 cm^{-1} in Figure 2 shows a slight downward energy shift when $^{18}O_2$ is loaded on the Al_2O_3 support. A downward energy shift is also observed for the peak around 3697 cm^{-1} when ^{18}O is loaded on the Al_2O_3 support. The hydroxyl peak at about 3734 cm^{-1} appears unchanged on the two isotopic catalyst samples, creating ambiguity in interpreting energy shifts in this region. In no case did we observe a detectable downward energy shift when isotopic oxygen was bonded to Pd.

We performed similar in situ FTIR spectroscopy experiments during CH_4 + $^{16}O_2$ combustion over $Pd^{16}O$/MCM-41 and $Pd^{18}O$/MCM-41. Figure 3 reveals that there is no detectable downward IR vibrational energy shift using $Pd^{18}O$/MCM-41 in comparison to using $Pd^{16}O$/MCM-41, under our reaction conditions. As with the alumina-based catalysts, we are unable to distinguish the accumulation of hydroxyls on Pd from those on the MCM-41 support around 3735 cm^{-1}.

dx.doi.org/10.1021/jp212236e | J. Phys. Chem. C XXXX, XXX, XXX−XXX

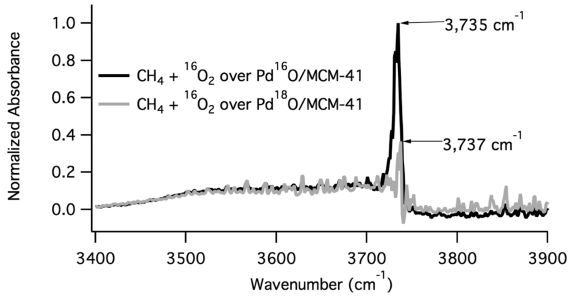

Figure 3. FTIR transmission spectra with 2 cm^{-1} resolution in the hydroxyl region during methane combustion over 3 wt % $Pd^{16}O$/MCM-41 and $Pd^{18}O$/MCM-41 at 325 °C.

The hydroxyl peak in Figure 3 shows lower intensity on the $Pd^{18}O$/MCM-41 catalyst compared to the $Pd^{16}O$/MCM-41 catalyst due to lower catalytic activity. The reduced activity on the $Pd^{18}O$/MCM-41 catalyst is due to its synthesis process, which included the reduction of $Pd^{16}O$/MCM-41 with hydrogen, and then reoxidation with $^{18}O_2$ to form $Pd^{18}O$/MCM-41. That process resulted in water formation on the catalyst, which was not fully desorbed after calcination by continuous flow of $^{18}O_2$ in He at 430 °C for two hours. While the $Pd^{16}O$/MCM-41 catalyst was heated to 540 °C prior to methane combustion, the isotopic catalyst was only heated to 430 °C in order to prevent isotopic oxygen exchange with the MCM-41 support. The FTIR spectra from methane combustion over the $Pd^{18}O$/MCM-41 sample shows numerous small peaks over the entire hydroxyl region, which confirms that water was not fully desorbed from the catalyst prior to reaction, and accounts for its lower catalytic activity

Though we were not able to distinguish hydroxyl accumulation on Pd from hydroxyl accumulation on the supports, we did find evidence to confirm the widely observed correlation between hydroxyl accumulation and catalytic deactivation This correlation is illustrated in Figure 4.

Figure 4 shows results from our in situ FTIR experiments at 325 °C in which CH_4 combustion over the Pd-based catalysts was performed, and then CH_4 gas flow was stopped while CH_4, CO_2, and hydroxyl/water desorption continued to be monitored. Normalized peak areas from CH_4, CO_2, and hydroxyl IR vibrational energy regions over time are shown. Methane and hydroxyl species are normalized to their respective maximum peak areas. Carbon dioxide is normalized to its maximum concentration, excluding the rise in the CO_2 spectra just after CH_4 gas flow was stopped. At that time, residual CH_4 in the gas line continued to react with oxygen but with increased residence time due to the slower total gas flow through the reactor. This caused a temporary but significant surge in CO_2 product after the methane gas source was turned off.

For all tested catalyst materials shown in Figure 4, the rate of hydroxyl desorption after CH_4 flow was stopped is slower than the rates of CO_2 and CH_4 desorption. Catalytic deactivation during reaction occurred on the Pd/Al_2O_3 and Pd/MgO samples, corresponding to declining CO_2 output during the CH_4 combustion period. Catalytic deactivation on these catalysts is shown to correlate with hydroxyl accumulation during reaction, which is slow to desorb. Hydroxyl accumulation is likely to have been responsible for catalyst poisoning and deactivation.

During reaction, we observe that the rate of catalytic deactivation is dependent on the support. The PdO/Al_2O_3 and PdO/MgO catalysts show unique patterns of short-term deactivation. The PdO/TiO_2 and PdO/MCM-41 catalysts do not show catalytic deactivation within the 20 min time frame of the reaction, though deactivation may occur over a longer time frame.[17] On the PdO/MCM-41 catalyst, the increasing CO_2 peak area during the reaction time frame may reflect the low

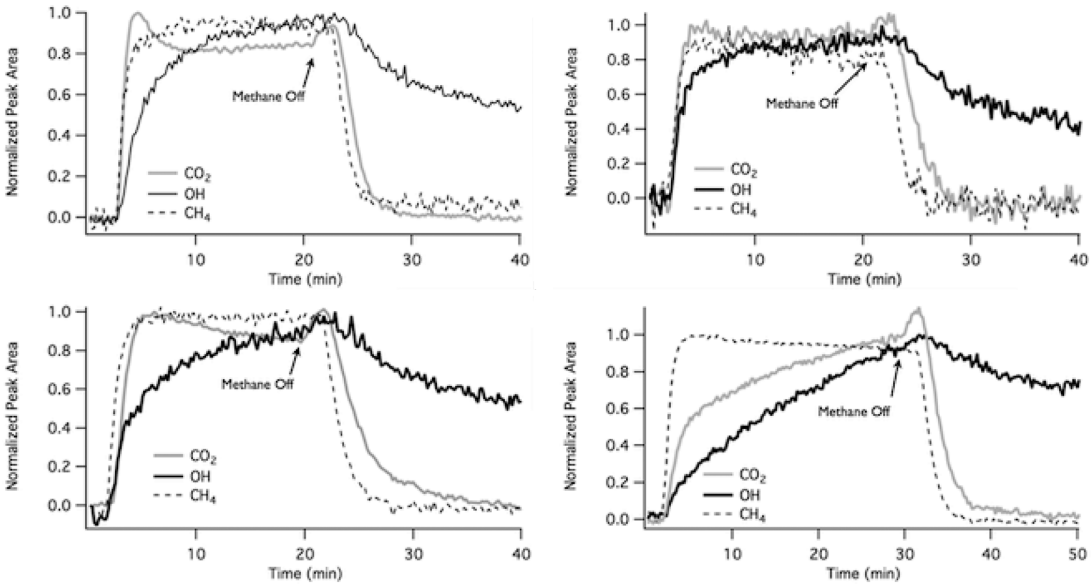

Figure 4. FTIR time series analysis during and after catalytic methane combustion at 325 °C. Normalized peak areas from CH_4, CO_2, and hydroxyl IR vibrational energy regions vs time. Catalysts are 3 wt % Pd/Al_2O_3 (top left), 3 wt % Pd/TiO_2 (top right), 3 wt % MgO (bottom left), and 3 wt % Pd/MCM-41 (bottom right).

dx.doi.org/10.1021/jp212236e | J. Phys. Chem. C XXXX, XXX, XXX–XXX

oxygen mobility on MCM-41 and correspondingly longer time frame for CO_2 to bind to the surface of the catalyst. Additionally, the methane combustion reaction over the MCM-41-based catalyst may be initially hindered due to diffusion limitations associated with the high surface area structure of MCM-41.

Each support in Figure 4 has a different surface area, with MCM-41 having substantially more surface area than the other supports. (See Table 1.) The hydroxyl accumulation per unit surface area for PdO/MCM-41 is correspondingly less than the hydroxyl accumulation per unit surface area on the other catalysts. This may account for the relatively slow rate that hydroxyls desorb from the PdO/MCM-41 catalyst in comparison to the other catalysts shown in Figure 4.

Figure 4 illustrates that there are multiple factors that influence catalytic activity during methane combustion, including the role of the support. Where catalytic deactivation occurs, it is associated with hydroxyl accumulation on the surface of the catalyst material.

In a prior study of the mechanism for methane combustion over PdO-based catalysts,[11] we proposed that gas phase oxygen dissociates and exchanges with oxygen on the support, and that Pd active catalytic sites are reoxidized with oxygen from the support during the catalytic reaction. This proposed component of the combustion mechanism reveals the possibility that a primary cause for catalytic deactivation under our experimental conditions is hydroxyl accumulation on the support, which hinders the oxygen migration and exchange process.

This hypothesis is supported by the results shown in Figure 5, which illustrate the impact of the presence of water on oxygen exchange with the support, in the absence of methane. We injected water into a 4% $^{18}O_2$ in He gas feed flowing toward catalyst samples that were heated to 400 °C. For each catalyst, $Pd^{18}O/Al_2{}^{16}O_3$ and $Pd^{18}O/Mg^{16}O$, oxygen exchange with the support is hindered by the presence of water. Oxygen exchange recovers when water is turned off. Recovery is faster on the MgO supported catalyst than the Al_2O_3 supported catalyst. The different oxygen exchange activity may be related to the difference in surface area of each of the supports. Our MgO support has an estimated surface area of 813 m^2/g, while the Al_2O_3 support has an estimated surface area of 480 m^2/g. (See Table 1.) The higher surface area of the MgO support suggests that active sites for oxygen exchange will become exposed more quickly as water desorbs from its surface.

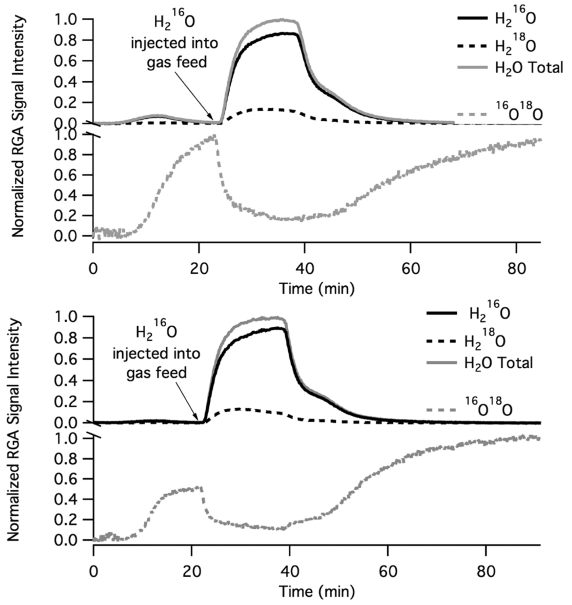

Figure 5. Mass spectrometer output from $^{18}O_2$ flowing over $Pd^{18}O/Al_2{}^{16}O_3$ (top) and $Pd/^{18}O/Mg^{16}O$ (bottom) at 400 °C. Water was injected during oxygen exchange with the catalyst supports. Its impact on oxygen exchange with the support is shown by the changes in $^{18}O^{16}O$ output.

Prior to the injection of water into the gas flow, a syringe was inserted into a septum in preparation for the water injection. At that time, there was an increase in detected $^{16}O_2$. However, there was no correlation between the increased $^{16}O_2$ level, the water concentration, or the decrease in $^{16}O^{18}O$ when water was injected into the gas flow. Thus, the $^{16}O^{18}O$ concentration profile is not attributable to the introduction of $^{16}O_2$ during the water insertion process.

A relationship between oxygen surface mobility and the rate of catalytic deactivation can also be seen in Figure 4, where the rate of deactivation, as measured by the decline in CO_2 peak area over time, is faster on 3 wt % PdO/Al_2O_3 in comparison to the rate of deactivation on 3 wt % PdO/MgO. The rate of deactivation is slower on the catalyst having the greater oxygen surface mobility (PdO/MgO). This supports the finding by Ciuparu et al. that the greater the support's oxygen surface mobility, the greater the resistance to water inhibition of the catalytic reaction.[10] However, we note that the relationship between increasing oxygen mobility and decreasing rate of catalytic deactivation is complex. Silica, the material that composes MCM-41, has lower oxygen mobility than both MgO and Al_2O_3; yet, during the time frame of our deactivation experiments (Figure 4), there was no evidence of deactivation on the PdO/MCM-41 catalyst.

CONCLUDING REMARKS

Catalytic deactivation over Pd-based catalysts during methane combustion in the temperature regime below 450 °C, in a fuel lean environment, is associated with hydroxyl accumulation on the oxide supports. Hydroxyl accumulation on the supports inhibits oxygen exchange with the supports, which suggests that oxygen is inhibited from migrating between PdO/Pd and the support. It follows that hydroxyl accumulation on the support prevents oxygen from the support from migrating to active Pd sites and participating in the catalytic combustion reaction. Hydroxyl accumulation on the catalyst also hinders the catalytic combustion reaction by blocking active catalytic sites. A Pd–OH bond may exist at around 3734 cm^{-1}. However, this finding is inconclusive due to the overwhelming accumulation of hydroxyls on the metal oxide supports.

Catalytic deactivation observed in this investigation is only partial and can be explained by the existence of multiple pathways for oxygen to react with methane on the catalyst surface, including oxygen from the gas phase, oxygen from PdO, and oxygen from the support through exchange with the catalyst.

ASSOCIATED CONTENT

Supporting Information

Available catalyst characterization information includes H_2 TPR data, TEM images and related particle size distribution data,

dx.doi.org/10.1021/jp212236e | J. Phys. Chem. C XXXX, XXX, XXX–XXX

and X-ray diffraction data for each of the catalyst materials used in this study. Also included is FTIR data showing hydroxyl peak shift of about 7 cm^{-1} when isotopic oxygen is loaded on Pd/Al_2O_3. This material is available free of charge via the Internet at http://pubs.acs.org.

AUTHOR INFORMATION

Corresponding Author
*E-mail: bill.schwartz@yale.edu.

Notes
The authors declare no competing financial interest.

ACKNOWLEDGMENTS

We thank the Environmental Protection Agency and the Petroleum Research Fund for their support of this work. We also gratefully acknowledge the assistance and advice provided by Gary Haller and Charles McEnally of Yale University.

REFERENCES

(1) Burch, R.; Urbano, F. J.; Loader, P. K. *Appl. Catal., A* **1995**, *123*, 173−184.
(2) Burch, R. *Catal. Today* **1997**, *35*, 27−36.
(3) Ribeiro, F. H.; Chow, M.; Dallabetta, R. A. *J. Catal.* **1994**, *146*, 537−544.
(4) Roth, D.; Gelin, P.; Primet, M.; Tena, E. *Appl. Catal., A* **2000**, *203*, 37−45.
(5) Gao, D. N.; Wang, S.; Zhang, C. X.; Yuan, Z. S.; Wang, S. D. *Chin. J. Catal.* **2008**, *29*, 1221−1225.
(6) Van Giezen, J. C.; Van den Berg, F. R.; Kleinen, J. L.; Van Dillen, A. J.; Geus, J. W. *Catal. Today* **1999**, *47*, 287−293.
(7) Ciuparu, D.; Katsikis, N.; Pfefferle, L. *Appl. Catal., A* **2001**, *216*, 209−215.
(8) Ciuparu, D.; Pfefferle, L. *Appl. Catal., A* **2001**, *209*, 415−428.
(9) Burch, R.; Urbano, F. J.; Loader, P. K. *Appl. Catal., A* **1995**, *123*, 173−184.
(10) Ciuparu, D.; Perkins, E.; Pfefferle, L. *Appl. Catal., A* **2004**, *263*, 145−153.
(11) Schwartz, W. R.; Ciuparu, D.; Pfefferle, L. D. *J. Phys. Chem. C* **2012**, DOI: 10.1021/jp2119668.
(12) Schneider, M.; Duff, D. G.; Mallat, T.; Wildberger, M.; Baiker, A. *J. Catal.* **1994**, *147*, 500−514.
(13) Jenkins, R.; Snyder, R. L. *Introduction to X-ray Powder Diffractometry*; Wiley: New York, 1996.
(14) Muller, C. A.; Maciejewski, M.; Koeppel, R. A.; Baiker, A. *J. Catal.* **1997**, *166*, 36−43.
(15) Knözinger, H.; Ratnasamy, P. *Catal. Rev. Sci. Eng.* **1978**, *17*, 31−70.
(16) Morterra, C.; Magnacca, G. *Catal. Today* **1996**, *27*, 497−532.
(17) Yin, F. X.; Ji, S. F.; Wu, P. Y.; Zhao, F. Z.; Li, C. Y. *J. Catal.* **2008**, *257*, 108−116.
(18) Ciuparu, D.; Bozon-Verduraz, F.; Pfefferle, L. *J. Phys. Chem. B* **2002**, *106*, 3434−3442.
(19) Guerrero, S.; Araya, P.; Wolf, E. E. *Appl. Catal., A* **2006**, *298*, 243−253.